http://dx.doi.org/10.5012/bkcs.2012.33.12.4074

Mechanism Studies of Substituted Triazol-1-yl-pyrimidine Derivatives Inhibition on *Mycobacterium tuberculosis* Acetohydroxyacid Synthase

Pham Ngoc Chien, In-Pil Jung, Katta Venugopal Reddy,† and Moon-Young Yoon*

Department of Chemistry and Institute of Natural Sciences, Hanyang University, Seoul 133-791, Korea
**E-mail: myyoon@hanyang.ac.kr*
†Department of Chemistry, Vikrama Simhapuri University, Nellore-524001, India
Received July 3, 2012, Accepted September 19, 2012

The first step in the common pathway for the biosynthesis of branched chain amino acids is catalyzed by acetohydroxyacid synthase (AHAS). The AHAS is found in plants, fungi and bacteria. With an aim to identify new *anti*-tuberculosis drugs that inhibit branched chain amino acid biosynthesis, we screened a chemical library against *Mycobacterium tuberculosis* AHAS. The screening identified four compounds, AVS 2087, AVS 2093, AVS 2236, and AVS 2387 with IC_{50} values of 0.28, 0.21, 3.88, and 0.25 μM, respectively. Moreover, these four compounds also showed strong inhibition against reconstituted AHAS with IC_{50} values of 0.37, 0.26, 1.0, and 1.18 μM, respectively. The basic scaffold of the AVS group consists of 1-pyrimidin-2-yl-1*H*-[1,2,4]-triazole-3-sulfonamide. The most active compound, AVS 2387, showed the lowest total interaction energy –8.75 Kcal/mol and illustrates its binding mode by hydrogen bonding with Hε of Gln517 with the distance of 2.24 Å.

Key Words : Acetohydroxyacid synthase, Docking, *Mycobacterium tuberculosis*, Tuberculosis, Triazol-1-yl-pyrimidines

Introduction

Acetohydroxyacid synthase (AHAS) catalyzes the first step in the common pathway of the biosynthesis of the branched chain amino acids (BCAAs), valine, leucine and isoleucine. AHAS catalyzes the condensation of two molecules of pyruvate to form acetolactate in the biosynthesis of valine and leucine, or the condensation of pyruvate and 2-keto-butyrate to form 2-aceto-2-hydroxybutyrate in the biosynthesis of isoleucine.[1] AHAS is found in bacteria, fungi, algae and higher plants but not in animals. Biochemical studies have shown that AHAS requires three cofactors: ThDP (Thiamine diphosphate) and a bivalent metal ion such as Mg^{2+} or Mn^{2+}, for its activity, and flavin adenine dinucleotide (FAD) for structural integrity.[2,3] The bacterial AHASs are generally composed of catalytic subunits with a molecular weight of about 60 kDa and small regulatory subunits with molecular weight of 9-19 kDa which are required for full activity and for sensitivity to feedback inhibition by valine in a hetero-tetrameric α2β2 structure. The holoenzymes of AHAS, reconstituted from purified subunits has previously been demonstrated not to be significantly different from the native protein.[4-6]

Tuberculosis is a chronic disease caused by intracellular infection with *Mycobacterium tuberculosis*.[7] Tuberculosis is responsible for the death of more people each year than any other single infectious disease, with 7 million new cases and million deaths annually.[8] Tuberculosis is a major health challenge even in the developed world because of the spread of strains with multiple drug resistance, and considerable effort is currently being invested in the search of new drugs.[8] Previous studies have been shown that BCAAs auxotrophic strain of mycobacterium failed to proliferate because of the inability to use amino acids from their hosts, indicating that inhibitors for the BCAAs biosynthesis could be used as *anti* mycobacterium agents.[9,10] However, several classes of widely and safely used commercial herbicides such as the sulfonylureas and the imidazoliones are inhibitors of AHAS.[11,12] Subsequently, several other compounds that inhibit AHAS but are not yet commercially available as herbicides were reported and reviewed elsewhere.[13] These inhibitors inhibit growth of several bacterial strains by inhibiting AHAS activity, and the absence of AHAS in animals makes it an even more attractive target when developing antimicrobial agents.[13]

In this study, we have individually expressed, purified, and reconstituted the catalytic and regulatory subunits of *M. tuberculosis* AHAS (Mtb-AHAS). A high-throughput screening was carried out against the catalytic subunit of Mtb-AHAS with the goal of developing *anti*-tuberculosis agents. In addition, the inhibition kinetics and binding modes of candidate chemicals were analyzed against the Mtb-AHAS.

Materials and Methods

Materials. Bacto Tryptone, yeast, and Bacto Agar were purchased from Difco Laboratories (Sparks, NV, USA). Sodium pyruvate, FAD, ThDP, $MgCl_2$, IPTG (isopropyl-β-D-thiogalactoside), creatine, and α-naphthol were obtained

Abbreviations: AHAS, acetohydroxyacid synthase; BCAA, branched-chain amino acid; Mtb, *Mycobacterium tuberculosis*; ProSA, Protein Structure Analysis

from Sigma Chemical Co. (St. Louis, MO, USA). *E. coli* strain, DH5α and BL21 (DE3), were from Novagen. All other chemicals were obtained from commercial sources and were of the highest quality available. KSW and KHG chemicals were obtained from the Korean Institute of Science and Technology (KIST, Seoul, Korea). AVS series compounds were obtained from the Korean Chemical Bank (KRICT, Daejeon, Korea).

Expression, Purification and Reconstitution of Mtb-AHAS. The cloning, expression and purification of both catalytic and regulatory subunits of Mtb-AHAS was carried out as described previously.[14] The initial reconstitution experiments were conducted at a fixed concentration of catalytic subunit (0.5 μg) and varied concentrations of regulatory subunit (0-10 μg). Purified catalytic and regulatory subunits were incubated for 15 min at 37 °C in a 100 mM potassium phosphate buffer (pH 8.0), containing 10 mM $MgCl_2$, 1 mM ThDP, and 50 μM FAD. The reaction was initiated by the addition of 100 mM pyruvate, and the AHAS activity was assayed by colorimetric assay, as described previously.[14]

Screening of Mtb-AHAS Inhibitors. To identify novel inhibitors of Mtb-AHAS, a high throughput screening of a chemical library was performed against catalytic subunit, as described previously.[14] For the inhibition study, all chemicals were dissolved in dimethyl sulfoxide (DMSO). The inhibition activity of selected compounds was further analyzed against the holoenzyme activity. Unless otherwise noted, all holoenzyme experiments were performed with a 15 min incubation of 0.5 μg of catalytic subunit and 10 μg of regulatory subunit, in standard assay buffer. All kinetic studies were performed using a discontinuous colorimetric assay, with the inhibitors in various concentrations, as appropriate for the particular experiment.

Preparation of the Model of Mtb-AHAS. The amino acid sequence of Mtb-AHAS was obtained from the NCBI database (Accession number YP_177917). The structure of Mtb-AHAS was erected by comparative modeling using the program Modeller9v2.[15] The template was obtained by the similarity search by BLAST. This elucidates 3E9Y (*A. thaliana* AHAS) as template. The structure was modeled by using this template and minimized (1200 steps of steepest descent) using GROMACS 3.3.3.[16] The obtained model was then evaluated by Protein Structure Analysis (ProSA) and Procheck.

Molecular Docking. The docking studies of the modeled protein with the AVS compounds were performed by using Autodock 4.0.[17,18] The modeled protein was initially standardized by adding polar hydrogens, kollman charges and atom type. Further it was kept rigid in the docking process, where the ligand was prepared flexible with all possible torsions by the ligand module in Auto Dock Tools (ADT). The docking area was defined by a box which had the grid points of 101 Å × 101 Å × 101 Å with 0.375 Å spacing. This fixation was utilized to define the atom types of the ligand by the AutoGrid. A total of 50 conformations were generated by using the Lamarckian genetic algorithm local search method. For local search the Solis and Wets algorithm was applied using a maximum of 300 iterations. The energy evaluation was set to 2.5×10^7 with the maximum of 2.7×10^4 generations. The population size was set to 150 with a mutation rate of 0.02 and a cross over rate of 0.8 for all the generations of docking process. At the end of the docking all the conformations were clustered based on the root mean square deviation (RMSD) of the ligand conformations and ranked based on the lowest binding free energy.

Results

Expression, Purification and Reconstitution of Mtb-AHAS. The expressed protein was highly soluble and purified to more than 95% homogeneity using His-tag affinity chromatography. The molecular weight of the catalytic and regulatory subunit of purified Mtb-AHAS was measured as approximately 63 kDa and 20.4 kDa by SDS-PAGE (data not shown). The specific activity of isolated catalytic subunits was calculated to be of 2.4 U/mg. Reconstitution with the regulatory subunit yielded a 1.45 fold increase in specific activity. Activity as a function of regulatory subunit concentration is shown in Figure 1.

Screening of Mtb-AHAS Inhibitors. To identify small molecule inhibitors against the Mtb-AHAS, a discontinuous colorimetric assay method, which is suitable for high throughput screening, was performed with a chemical library of 226 random structured compounds. The screening identified four structurally related hit compounds (AVS2087, AVS2093, AVS2236, and AVS2397) that inhibited the enzyme activity of the catalytic subunit by more than 98% at the concentration of 100 μM. The 50% inhibition concentration (IC_{50}) was analyzed by fitting to Eq. (1), where V_0 is the reaction rate without inhibitor, V_f is the rate at maximal inhibition and [I] is an inhibitor concentration

$$v = \frac{(V_0 - V_f) \times IC_{50}}{IC_{50} + [I]} + V_f \quad (1)$$

In a dose-dependent manner, the AVS2087, AVS2093,

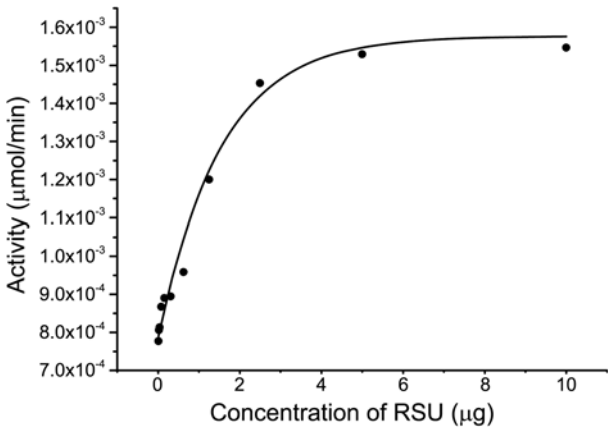

Figure 1. Reconstitution of Mtb-AHAS holoenzyme by increasing concentrations of the regulatory subunit. Assays contained (0.5 μg) of catalytic and varying concentrations of the regulatory subunit as shown.

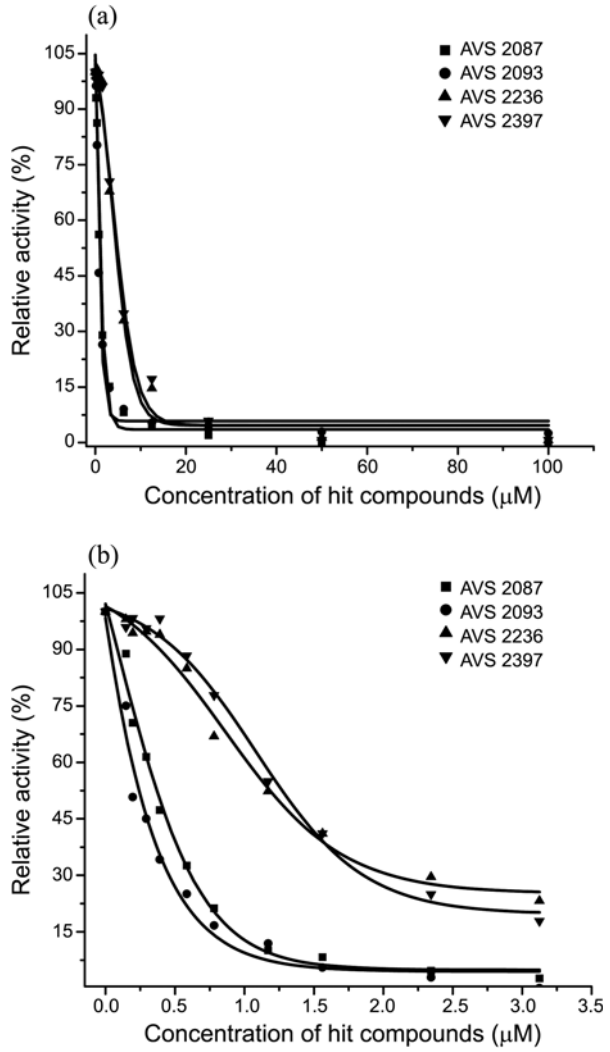

Figure 2. The relative activity of the catalytic subunitof Mtb-AHAS (a) and holoenzyme (b) as a function of inhibitor concentration. The IC_{50} values were mentioned at Table 1.

AVS2236, and AVS2387 compounds inhibited Mtb-AHAS with IC_{50} values of 0.28, 0.21, 3.88 and 2.50 μM respectively (Fig. 2(a) and Table 1). These four compounds also showed strong inhibition against the reconstituted AHAS with IC_{50} values of 0.37, 0.26, 1.0, and 1.18 μM, respectively (Fig. 2(b) and Table 1). The main scaffold of these novel compounds consists of a 1,2,4-triazole-3-sulfonamide with different substituted groups; AVS2087, with 1-(4,6-dimethoxy-2-pyrimidinyl), 5-methyl, and *N*-(2-isopropyl-6-nitrophenyl) substituted groups; AVS2093, with 1-(4,6-dimethoxy-2-pyrimidinyl), 5-methoxymethyl, and *N*-(2-isopropyl-6-nitrophenyl) substituted groups; AVS2236, with 1-(4-chloro-6-methoxy-2-pyrimidinyl), 5-methoxy, and *N*-(2-methyl-6-nitrophenyl) substituted groups; and AVS2387, with 1-(4,6 dimethoxy-2-pyrimidinyl),5-methylthio, and *N*-(2-chloro-6-fluorophenyl) substituted groups (Table 2).

Inhibition Kinetics. The inhibition mechanisms of the most potent inhibitors were selected for further study. Initial rates in the presence of inhibitors were measured as a function of pyruvate concentration at fixed inhibitor concentrations (data not shown). The K_{ii} and K_{is} values were determined by fitting the data to Eqs. (2) or (3), for noncompetitive and uncompetitive inhibition, respectively.

$$v = V_{max} \times [S]/\{K_m (1+ [I]/K_{is} + [S] (1 + [I]/K_{ii}\} \quad (2)$$

$$v = V_{max} \times [S]/\{K_m + [S] (1 + [I]/K_{ii})\} \quad (3)$$

In these Eqs. [S] and [I] are the concentrations of substrate and inhibitor. K_{is} is the inhibition constant derived from the slope, whereas K_{ii} is the constant derived from the intercepts of 1/V *vs* 1/S plots. The results showed that AVS2093 was uncompetitive inhibition against both the catalytic subunit and reconstituted Mtb-AHAS. Three other chemicals (AVS2087, AVS2236, and AVS2397) were noncompetitive inhibitors against both the catalytic subunit and reconstituted Mtb-AHAS. The K_{ii} and K_{is} values indicated the inhibition potency of AVS chemicals against Mtb-AHAS were shown in Table 1.

Homology Modeling. The amino acid sequence of Mtb-AHAS shown 47% identity and 62% sequence similarity with *A. thaliana*-AHAS (3E9Y) on similarity search. The 3E9Y was fixed as the template to model the Mtb-AHAS

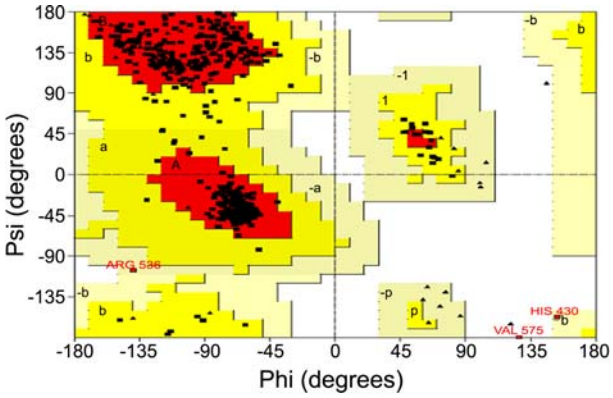

Figure 3. Ramchandran plot of the homology-modeled Mtb-AHAS.

Table 1. Inhibition kinetics of AVS chemicals against the catalytic subunit and holoenzyme of Mtb-AHAS

Inhibitor	IC_{50} (μM)		K_{is} (μM)		K_{ii} (μM)	
	Catalytic subunit	Holoenzyme	Catalytic subunit	Holoenzyme	Catalytic subunit	Holoenzyme
AVS 2087	0.28 ± 0.02	0.37 ± 0.03	0.26 ± 0.01	0.23 ± 0.63	0.06 ± 0.01	0.94 ± 0.86
AVS 2093	0.21 ± 0.05	0.26 ± 0.06	0.42 ± 0.14	1.21 ± 0.29	1.14 ± 0.24	0.96 ± 0.45
AVS2236	3.88 ± 0.17	1.00 ± 0.04	0.55 ± 0.21	1.11 ± 0.40	0.24 ± 0.20	1.64 ± 0.6
AVS2387	2.50 ± 0.08	1.18 ± 0.09	0.36 ± 0.67	ND	0.94 ± 0.16	1.29 ± 0.66

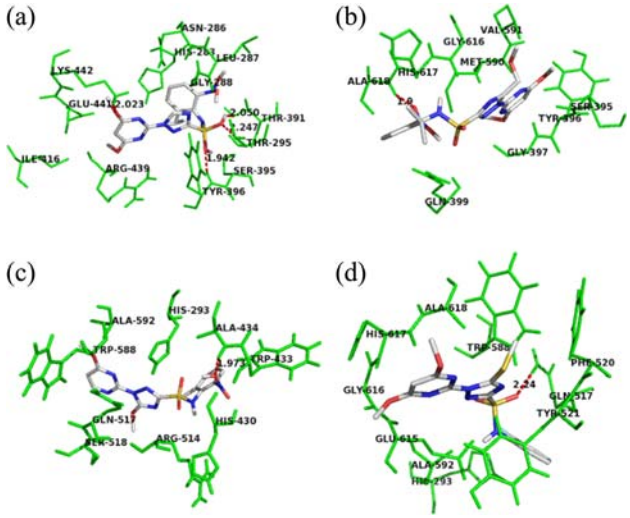

Figure 4. Binding modes of AVS chemicals in Mtb-AHAS (a) AVS2087; (b) AVS2093; (c) AVS2236; (d) AVS2387.

structure by using Modeller program.[15] The model was reliable by its distribution over the Ramachandran plot where 97.9% of residues were found in allowed regions (Fig. 3). The ProSA analysis demonstrated the modeled structure's quality by its Z – score of −8.5. The possible ligand binding region on the protein was found by Q-finder server. This region was further used to get best binding in the docking process.

Molecular Docking. After the addition of appropriate charges and hydrogens, the docking was carried out with a proper grid. The lowest-energy conformer was chosen for further analysis from among the 50 runs. The AVS2087 shows interaction with the protein at four places with a binding free energy of −8.63 kcal/mol. Thr295 and Tyr396 donates its side chain and main chain hydrogen to O3 of the ligand and forms the hydrogen bond with the distance of 2.247 and 1.945 Å respectively (Fig. 4(a)). Further Thr391 forms hydrogen bond by accepting the H10 by its side chain oxygen (OG1) with the distance of 2.241 Å, whereas the Lys442 interacts with O2 of the ligand by donating its hydrogen forms bonding with the distance of 2.023 Å. Other residues which are in van der Waals contact with the docked ligand were screened in the Table 2. The AVS2093 and AVS2236 interact with the protein by binding with its Hη (main chain hydrogen) of Ala618 and Ala434 respectively (Fig. 4(b) and Fig. 4(c)). The AVS2093 and AVS2236 show the binding free energy of −7.82 kcal/mol and −8.47 kcal/mol with the hydrogen bond distance of 1.9 and 1.943 Å, respectively. Subsequently, the AVS2387 illustrates its binding mode by hydrogen bonding with Hε of Gln517 with the distance of 2.24 Å (Fig. 4(d)). The other residues that interact with the ligand by van der Waals are shown in Table 2 and the binding modes of each ligand were shown in Figure 4.

Discussion

A variety of organisms such as plants, fungi, and bacteria can synthesize the essential BCAAs from their metabolites. Animals cannot perform this synthesis and have to obtain these essential amino acids from their diet. Therefore, the enzymes involved in BCAA biosynthesis have been accepted as potential enzyme targets for the development of herbicides, fungicides, and antimicrobial compounds. Over the past 30 years, several BCAA biosynthetic enzyme inhibitors have been studied in plants and used worldwide as popular herbicides.[11,12] However, antimicrobial drugs targeting AHAS

Table 2. Calculated binding energies and hydrogen bonding interactions for AVS chemicals in catalytic subunit of Mtb-AHAS

Ligand name	Structure	Binding energy (kcal/mol)	Hydrogen bond and length (Å)	van der Waals interaction residues (scaling factor = 1.00 Å)
AVS 2087	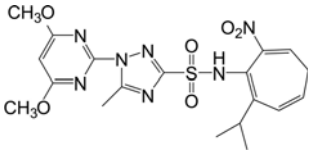	-8.63	THR 295: HG1 - O3 (2.247) TYR 396: HN - O3 (1.945) LYS 442 : HZ3 - O2 (2.023)	GLU441, LYS442, ILE416, ASN286, HIS283, GLY288, LEU287, ARG439, THR295, THR391, SER395, TYR396
AVS 2093	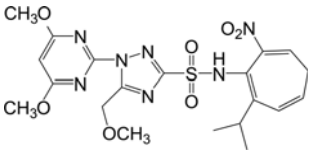	-7.82	ALA 816: HN -O6 (1.9)	ALA618, GLN399,GLY616, HIS617, MET590, VAL591, GLY397, TYR396, SER395
AVS 2236	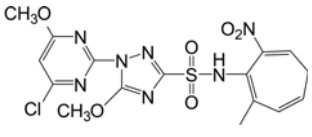	-8.47	ALA 434: HN - O5 (1.943)	TRP588, ALA592, GLN517, TRP433, ALA434, HIS430, ARG514, HIS293, SER518
AVS 2387	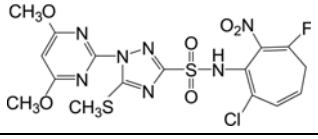	-8.75	GLN 517: HE - O1 (2.24)	HIS293, GLN517, TYR521, PHE520, ALA592, GLU615, GLY616, HIS617, ALA618, TRP588

have not yet been widely studied even though AHAS has been accepted as a new antimicrobial target enzyme.[13] In order to create an efficient tool for the design of new *anti*-tuberculosis drugs that inhibit BCAA biosynthesis, we screened and identified potential AHAS inhibitors. To characterize the new inhibitors of Mtb-AHAS, the individual subunits were expressed, and purified to homogeneity using the *E. coli* expression system. The purified individual subunits were reconstituted to form a holoenzyme, which had a specific activity higher than the purified catalytic subunit.

The plant AHAS inhibitors are emerged as widely used herbicides. In comparison to plant AHASs, the potency of herbicides inhibition is rather weak for bacterial AHASs.[13] Further, in comparison with plant AHASs, research on the development of bacterial AHAS inhibitors is very limited. Triazolopyrimidine is one of major classes of herbicides that targets plant AHAS.[19] In general, triazolopyrimidines consist of a di- or tri-substituted aromatic ring linked by a short bridge to a substituted triazolopyrimidine ring system. In the aromatic ring, an electron withdrawing group, like NO_2, is usually substituted in the aromatic ring at the ortho position. The novel compounds identified in this study (AVS 2087, AVS 2093, AVS 2236 and AVS 2397), substituted triazol-1-yl-pyrimidine derivatives, are similar with triazolopyrimidine, which has a 2-isopropyl-6-nitrophenyl group. However the main scaffold of this compound consists of 1-(4,6-dimethoxy-2-pyrimidinyl)-triazole-3-sulfonamide instead of the triazolopyrimidine ring system. This typical structure showed submicromolar level inhibition against Mtb-AHAS. The inhibition of AVS 2236 and AVS 2387 against holoenzyme were demonstrated to be better than catalytic subunit. However, the AVS 2087 and AVS 2093 showed similar IC_{50} values against both the holoenzyme and catalytic subunit. Moreover, AVS 2093 compound showed uncompetitive inhibition, where as the AVS 2087, AVS 2236 and AVS 2387 compounds noncompetitively inhibited both holoenzyme and catalytic subunit. The IC_{50} and inhibition kinetics suggest that AVS compounds are the most potent inhibitors of Mtb-AHAS than any other herbicides. In addition, these compounds also found to inhibit the various bacterial AHASs with similar sub-micromolar level inhibition.[20,21] Further, the molecular docking simulations of four AVS compounds with catalytic subunit of Mtb-AHAS revealed the details of their interactions. The docking data suggests the possible location of AVS compounds at different binding sites and exploits an inhibitory mechanism that can be instrumental in further developing inhibitors.

In summary, the substituted triazol-1-yl-pyrimidine derivatives were characterized as potent Mtb-AHAS inhibitors. The potent inhibition of these derivatives against various bacterial AHASs suggests that the triazol-1-yl-pyrimidine skeleton is a promising structural template for the development of novel bacterial AHAS inhibitors. The possible binding modes evaluated by molecular docking are of future interest in the design of novel *anti*-tuberculosis agents that inhibits Mtb-AHAS.

Acknowledgments. This research was supported by Basic Science Research Program through the National Research Foundation of Korea (NRF) funded by the Ministry of Education, Science and Technology (2012R1A1A2008516) and Rural Development Administration, Republic of Korea and Bio-industry Technology Development Program, Ministry for Food, Agriculture, Forestry and Fisheries, Republic of Korea (111079-3).

References

1. McCourt, J. A.; Duggleby, R. G. *Amino Acids* **2006**, *31*, 173.
2. Gedi, V.; Koo, B. S.; Kim, D. E.; Yoon, M. Y. *Bull. Korean Chem. Soc.* **2010**, *31*, 3782.
3. Kyoung, C. J.; Chien, P. N.; Sung, H.; Han, S. H.; Jung, C. D.; Kim, J.; Yoon, M. Y. *Bull. Korean Chem. Soc.* **2007**, *28*, 1109.
4. Vinogradov, V.; Vyazmensky, M.; Engel, S.; Belenky, I.; Kaplun, A.; Kryukov, O.; Barak, Z.; Chipman, D. M. *Biochim. Biophys. Acta* **2006**, *1760*, 356.
5. Hill, C. M.; Pang, S. S.; Duggleby, R. G. *Biochem J.* **1997**, *327*, 891.
6. Vyazmensky, M.; Sella, C.; Barak, Z.; Chipman, D. M. *Biochemistry* **1996**, *35*, 10339.
7. Murray, P. R.; Rosenthal, K. S.; Kobayashi, G. S.; Pfaller, M. A. *Medical Microbiology*, Mosby, St. Louis **1998**, 319.
8. Dye, C.; Scheele, S.; Dolin, P.; Pathania, V.; Raviglion, R. C. *JAMA* **1999**, *282*, 677.
9. Guleria, I.; Teitelbaum, R.; McAdam, R. A.; Kalpana, G.; Jacobs, W. R., Jr.; Bloom, B. R. *Nat. Med.* **1996**, *2*, 334.
10. Grandoni, J. A.; Mart, P. T.; Schloss, J. V. *J. Antimicrob. Chemother.* **1998**, *42*, 475.
11. LaRossa, R. A.; Schloss, J. V. *J. Biol. Chem.* **1984**, *259*, 8753.
12. Shaner, D. L.; Anderson, P. C.; Stidham, M. A. *Plant Physiol.* **1984**, *76*, 545.
13. Gedi, V.; Yoon, M. Y. *FEBS Journal* **2012**, *279*, 946.
14. Choi, K. J.; Yu, Y. G.; Hahn, H. G.; Choi, J. D.; Yoon, M. Y. *FEBS Lett.* **2005**, *579*, 4903.
15. Eswar, N.; Martin-Renom, M. A.; Webb, B.; Madhusudhan, M. S.; Eramian, D.; Shen, M.; Pieper, U.; Sali, A. *Curr. Protoc. Bioinformatics* **2006**, Chapter 5: Unit 5.6.
16. Berendsen, H. J. C.; Van der Spoel, D.; Van Drunen, R. *Comp. Phys. Comm.* **1995**, *91*, 43.
17. Morris, G. M.; Goodsell, D. S.; Halliday, R. S.; Huey, R.; Hart, W. E.; Belew, R. K.; Olson, A. J. *J. Comput. Chem.* **1998**, *19*, 1639.
18. Lee, J. S.; White, E.; Kim, S. G.; Kim, S. K. *Bull. Korean Chem. Soc.* **2010**, *31*, 3644.
19. Gerwick, B. C.; Subermanian, V. I.; Loney-Gallant, V. I.; Chander, D. P. *Pestic. Sci.* **1990**, *29*, 357.
20. Gedi, V.; Jayaraman, K.; Kalme, S.; Park, H. Y.; Park, H. C.; La, I. J.; Hahn, H. G.; Yoon, M. Y. *Biochim. Biophys. Acta* **2010**, *1804*, 1369.
21. Chien, P. N.; Moon, J. Y.; Cho, J. H.; Lee, S. J.; Park, J. S.; Kim, D. E.; Park, Y.; Yoon, M. Y. *Biosci. Biotechnol. Biochem.* **2010**, *74*, 2281.